Structural Engineering and Mechanics, Vol. 9, No. 5 (2000) 469-482
DOI: http://dx.doi.org/10.12989/sem.2000.9.5.469

Isolated RC wall subjected to biaxial bending moment and axial force

Honggun Park†

Department of Architecture, Seoul National University, San 56-1, Shinlim-Dong, Kwanak-Gu, Seoul 151-742, Korea

Abstract. A numerical study using nonlinear finite element analysis is performed to investigate the behavior of isolated reinforced concrete walls subjected to combined axial force and in-plane and out-of-plane bending moments. For a nonlinear finite element analysis, a computer program addressing material and geometric nonlinearities was developed. Through numerical studies, the internal force distribution in the cross-section is idealized, and then a new design method, different from the existing methods based on the plane section hypothesis was developed. According to the proposed method, variations in the interaction curve of the in-plane bending moment and axial force depends on the range of the permissible axial force per unit length, that is determined by a given amount of out-of-plane bending moment. As the out-of-plane bending moment increases, the interaction curve shrinks, indicating a decrease in the ultimate strength. The proposed method is then compared with an existing method, using the plane section hypothesis. Compared with the proposed method, the existing method overestimates the ultimate strength for the walls subjected to low out-of-plane bending moments, while it underestimates the ultimate strength for walls subject to high out-of-plane bending moments. The proposed method can address the out-of-plane local behavior of the individual wall segments that may govern the ultimate strength of the entire wall.

Key words: biaxial bending; compression; finite element; interaction curve; plasticity; reinforced concrete wall.

1. Introduction

For residential tall buildings up to 30 stories in Korea, the bearing wall-slab system is popular. The isolated reinforced concrete walls with long rectangular cross-sections are the essential structural elements in this bearing wall-slab system. The walls are subjected to considerable gravity load and lateral load due to wind and earthquake. Gravity and lateral loads induce axial forces and both in-plane and out-of-plane bending moments in the walls. According to ACI 318-95 (American Concrete Institute 1995) and the Korean Building Code for structural concrete, walls subject to combined flexure and axial loads can be designed in accordance with the provisions for compression members. These provisions are based on a design assumption that strains shall be directly proportional to the distance from the neutral axis. Current design methods for compression members are based on this assumption. Structural engineers also use the design methods for RC walls under combined biaxial bending moment and axial force.

However, it should be noticed that the assumption is applicable only to line members such as

† Assistant Professor

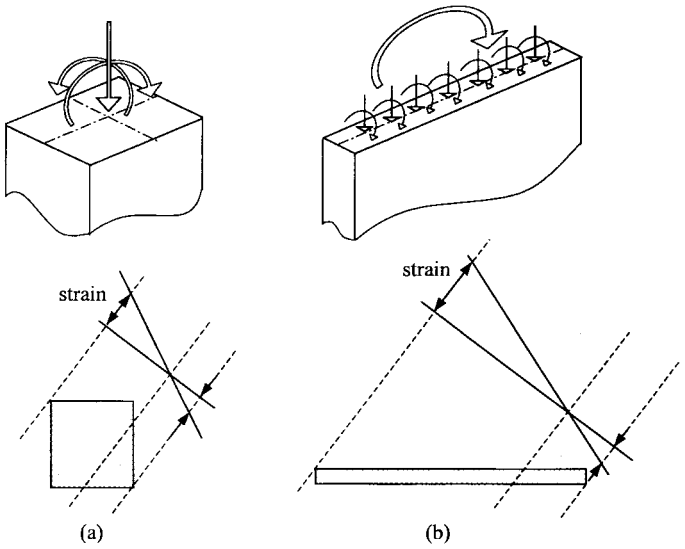

Fig. 1 Assumption of strain distribution for compression members under biaxial bending moments and axial force: (a) Reasonable assumption for column; (b) Unreasonable assumption for wall

columns, where the dimensions of the cross-section are much less than its length. For the line members, it is generally accepted that during flexural deformation, a plane of the cross-section remains plane, and that strains in the cross-section are directly proportional to the distance from the neutral axis (see Fig. 1a).

On the other hand, the wall with the long rectangular cross-section has very little out-of-plane bending stiffness, as compared with in-plane bending stiffness. Under biaxial bending moment, the skew neutral axis causes out-of-plane flexural deformations along the length. As a result, a distortion in the cross section occurs, and a plane section is not maintained during the deformation. This out-of-plane local behavior of the wall segments may govern the ultimate strength of the wall. In slender walls, for example, local buckling can occur in the compression zone (see Fig. 2).

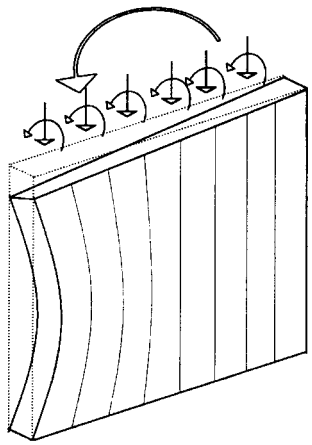

Fig. 2 Local buckling of slender wall under biaxial bending moments and axial force

Accordingly, the plane section hypothesis is no longer effective for the walls (see Fig. 1b). Current design methods using the plane section hypothesis could lead to an inaccurate estimation of the ultimate strength in the entire wall.

To the knowledge of the author, experimental studies for isolated walls with long rectangular cross sections that are subjected to combined axial force and biaxial bending moments have not yet been reported. Aoyama and Yoshimura (1980) did experimental studies for walls under biaxial bending moments without axial force. However, the cross-sections of the specimens are close to columns rather than walls. Although Huria *et al.* (1991) did numerical studies for barbell walls under axial force and biaxial bending moments, they also used the plan section hypothesis. There has yet been no discussion about whether the plane section hypothesis is applicable to isolated walls under these combined loads.

The primary goal of the study presented in this paper is to develop a design method for isolated walls under biaxial bending moment and axial force, which is different from the existing design methods based only on the plane section hypothesis. For this purpose, a computer program for nonlinear finite element analysis was developed. The internal force distribution in a cross-section of the wall was investigated by numerical studies, using the computer program. Then, a design method using an idealized distribution of internal forces is proposed.

2. Numerical model and implementation

A computer program addressing material and geometric nonlinearities was developed for studying the three-dimensional behavior of a wall subjected to combined in-plane and out-of-plane loads. For a material model of reinforced concrete, the unified method developed by Park and Klingner (1997) was used. The unified method combines plasticity and damage models. The concrete plasticity with multiple failure criteria addresses strength enhancement under multiaxial compression, and tensile cracking damage. The Drucker-Prager model is employed for the compressive and tensile failure criteria:

$$f_i=g_i(\sigma,J_2)-\bar{\sigma}_i(\varepsilon_{pi}) \qquad i=1, 2 \tag{1}$$

where

$$g_i(\sigma,J_2)=A_{i1}\sigma+A_{i2}\sqrt{3J_2}+A_{i3} \tag{2}$$

Here $g_i(\sigma,J_2)$ =effective stress; and $\bar{\sigma}_i$ =failure surface, which is the function of equivalent plastic strain, ε_{pi}. The subscripts i=1 and 2 indicate compressive crushing and tensile cracking, respectively. The constants, A_{i1}, A_{i2}, and A_{i3} can be determined using existing experimental results (Park and Klingner 1997). The compressive and tensile failure surface functions can be obtained from experimental uniaxial stress-plastic strain curves.

Associative flow and isotropic hardening are used for the stress-plastic strain relationships of both compressive crushing and tensile cracking. Total incremental plastic strain is defined by the sum of incremental plastic strains of both compressive crushing and tensile cracking:

$$\Delta\underline{\varepsilon}_p=\Delta\underline{\varepsilon}_{p1}+\Delta\underline{\varepsilon}_{p2} \tag{3}$$

Shell elements are used for the three-dimensional finite element analysis (see Fig. 3). For numerical integration over the volume of the element, 54 Gaussian points composed of 3×3 points

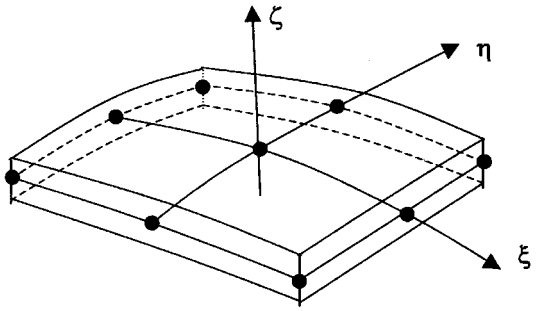

Fig. 3 Nine-node shell element

in the plane with 6 points over the thickness are used.

It is idealized that reinforcing steel has smeared properties in the plane where the reinforcing steel layer is placed. Tension stiffening stress induced by the interaction between cracked concrete and reinforcing steel is idealized by a combination of tension softening and bond stresses (Park and Klingner 1997). The bond stress is considered in the orientation of each reinforcement layer. For numerical integration, 3×3 Gaussian points are used in each reinforcing steel layer. Therefore, 36 Gaussian points are required for a wall with double layers of reinforcement in both vertical and horizontal directions.

The slenderness effect with respect to out-of-plane bending is also addressed. The Updated Lagrangian Formulation is used for the geometrical nonlinearity (Bathe 1982). At each loading step, the coordinates and the directional cosine vectors perpendicular to the tangent planes of the shell elements are updated by the corresponding displacements.

The solution strategies for nonlinear computation are described in a previous study (Park and Klingner 1997).

Since experiments for slender walls with long rectangular cross-sections subjected to both biaxial bending moments and axial compressive force have not been reported, it is difficult to verify the proposed numerical method. However, the same numerical method was also used in a study for flat plates subjected to combined in-plane compressive and out-of-plane loads (Park 1999). In the study, the proposed numerical method was verified by comparison with existing experiments of plates subjected to the combined loads. The study for flat plates is similar to the present study for the slender walls in that the two studies deal with a slender membrane under both in-plane and out-of-plane loads.

3. Numerical studies

3.1. Properties and finite element model of wall

Fig. 4 shows the dimensions and the properties of the wall to be studied. The wall measures 5,000-mm wide × 3,000-mm high × 200-mm thick. At the bottom, the wall is rigidly supported for all translational and rotational degrees of freedom except out-of-plane rotation. At the top, it is supported in the direction perpendicular to the face of the wall. For vertical reinforcement, 25-D13 (D13: As=127 mm^2) are uniformly distributed along the length at each face of the wall so that the

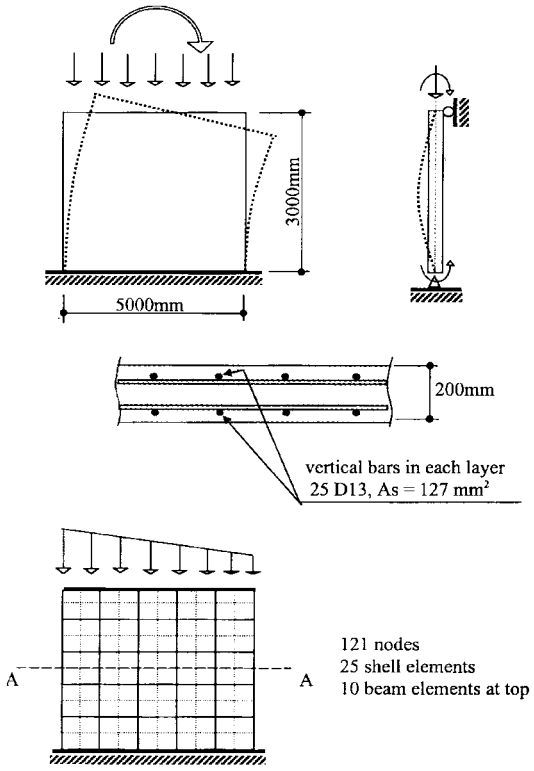

Fig. 4 Properties and finite-element model of wall

reinforcement ratio is 0.0063. The horizontal reinforcement ratio is the same as the vertical reinforcement ratio. The concrete cover for the reinforcing steel bars is 20 mm. The compressive strength of concrete is 30 MPa. The yield stress of the reinforcing steel bars is 400 MPa.

As shown in Fig. 4, the finite element model of the wall is composed of 121 nodes, 25 shell elements, and 10 beam elements. Axial forces and out-of-plane bending moments are uniformly distributed at the top of the wall. Out-of-plane bending moments with the opposite sign and the same magnitude are uniformly distributed also at the bottom. For in-plane bending moment, linearly distributed vertical forces are loaded on the top of the wall without horizontal forces so that shear forces do not affect its ultimate strength. The linearly distributed vertical forces are loaded on the rigid beams located at the top of the wall. The beams have infinite in-plane stiffness so that local damage due to the vertical forces does not occur near the top of the wall.

3.2. Wall under uniaxial bending moment and axial force

As a preliminary study for the wall under biaxial bending moment, and for verification of the proposed numerical model, numerical studies for a wall under both uniaxial bending moment and axial force were done. Figs. 5 and 6 show the numerical results. Fig. 5 shows the interaction curves of in-plane bending moment and axial force. Fig. 6 shows the interaction curves of out-of-plane bending moment and axial force. For verification of the numerical model, the numerical results were then compared with the interaction curves by PCACOL (Portland Cement Association 1992)

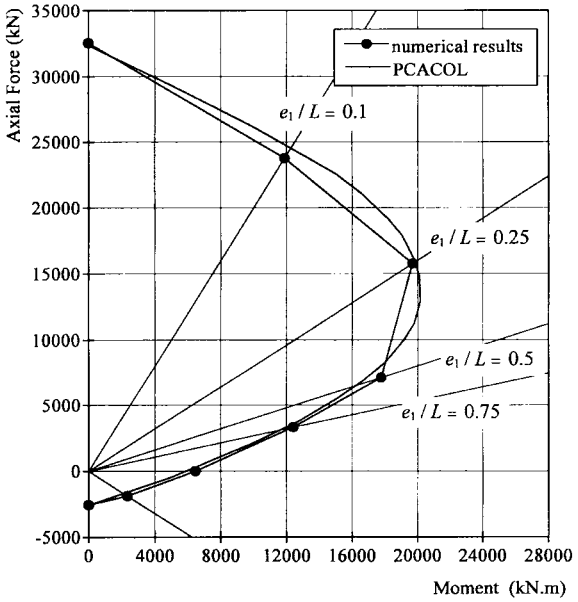

Fig. 5 Interaction curve of in-plane bending moment and axial force

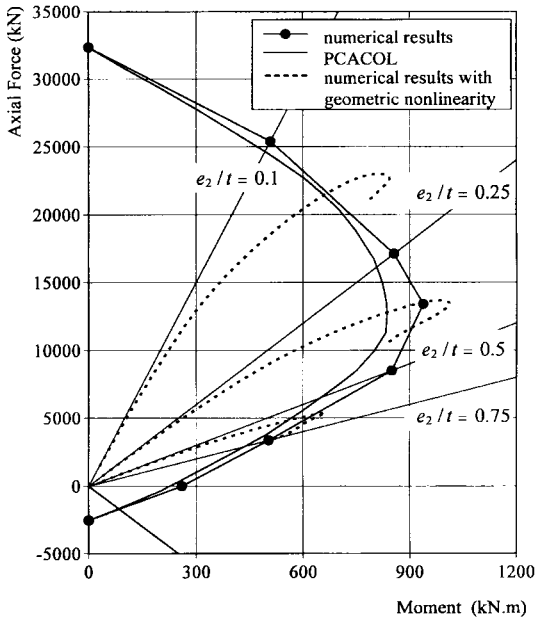

Fig. 6 Interaction curve of out-of-plane bending moment and axial force

that is commonly used for designing columns and walls. In the interaction curves by PCACOL, the parabolic curve with the maximum stress of f_c' is used for the compressive stress-strain relationship. In this paper, the positive sign indicates compression.

As shown in the figures, for in-plane bending moment, the numerical results agree with the interaction curve by PCACOL. For out-of-plane bending moment, on the other hand, the numerical results slightly overestimate the ultimate strength, near the balanced strain condition. Fig. 6 also shows the numerical results including the slenderness effect. The nonlinear curves of the eccentricity ratio (e_2/t) with the slenderness effect are compared with the linear eccentricity ratios without the slenderness effect.

3.3. Wall under biaxial bending moment and axial force

For a wall under biaxial bending moment and axial force, the loading path of the internal forces in the wall segments is conceptually presented in Fig. 7. At first, the wall is subjected to uniformly distributed axial force and out-of-plane bending moment. Subsequently, it is subjected to in-plane bending moment. The in-plane bending moment induces axial forces in the wall segments along the length of the wall. The axial forces are added to the external axial forces (see Fig. 7a). As a result, each wall segment can be idealized as a compression or tension member subjected to a combined out-of-plane bending moment and axial force.

In Fig. 7(b), the loading path of the internal force in the wall segments is shown in the interaction diagram of out-of-plane bending moment and axial force. Under this external out-of-plane bending moment and axial force, the internal force moves from O to C. In the compression zone where the subsequent in-plane bending moment induces compressive axial force, the internal force moves upward from C to A. In the tension zone, the internal force moves downward from C to B. As a

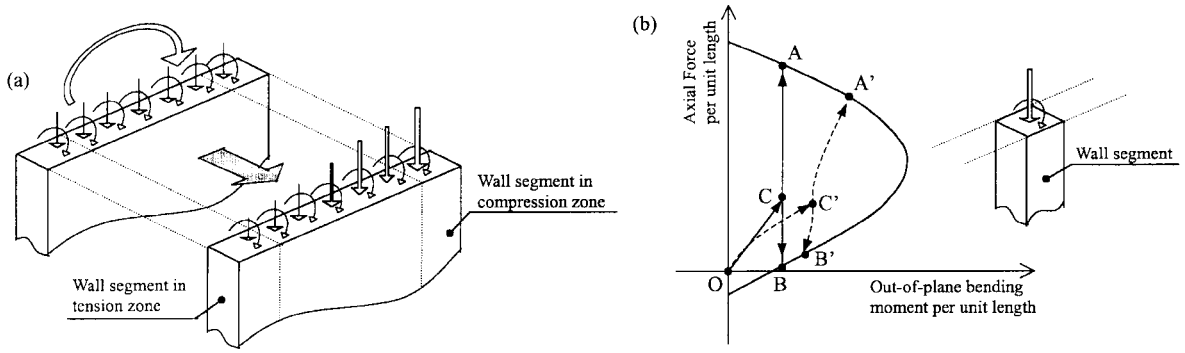

loading path		description
nonslender member	slender member	
O → C	O → C'	External compressive force and out-of-plane bending moment
C → A	C' → A'	Additional compressive force due to in-plane bending moment in compression zone
C → B	C' → B'	Additional tensile force due to in-plane bending moment in tension zone

Fig. 7 Wall segments subjected to out-of-plane bending moment and axial force: (a) Additional axial force induced by in-plane bending moment; (b) Loading path of internal force in the interaction curve of out-of-plane bending moment and axial force

result, the potential maximum and minimum axial forces correspond to A and B, respectively. All the internal forces in the wall segments exist on the loading path between A and B. Regardless of the amount of the out-of-plane bending moment, A belongs to the range of compression control, while B belongs to the range of tension control. If the internal force in the compression zone approaches A before the internal force in the tension zone approaches B, then a compressive crushing of concrete controls the ultimate strength. On the other hand, if the internal force in tension zone approaches B ahead, yielding of reinforcing steel controls the ultimate strength.

For slender members, the axial force magnifies the out-of-plane bending moment. Therefore, as shown in Fig. 7(b), all the internal forces exist on the curved loading path between A' and B'. The potential maximum and minimum axial forces also correspond to A' and B', respectively. It should now be noticed that the magnified bending moments at A' and B' correspond to the internal axial force including the external axial force and the contribution due to the in-plane bending moment. In the design of a compression member, generally, the moment magnification factor is determined by the external compressive force. However, the wall segments in the compression zone are subjected to the internal compressive force that is larger than the external compressive force. The moment magnification factor should be larger than that determined by the external force. Therefore, the out-of-plane bending moments in the individual wall segments should be magnified by the internal compressive force.

For verifying the loading path of the internal force, the following numerical studies were done. The wall is subjected to the uniform out-of-plane bending moment of 600 kNm (120 kN·m/m) or 300 kN·m (60 kN·m/m), accompanied by various magnitudes of axial forces. Then, the in-plane bending moment is increased up to the ultimate strength. Figs. 8(a) and (b) show the numerical results without and with geometric nonlinearity. The figures show the variations of the linearlized

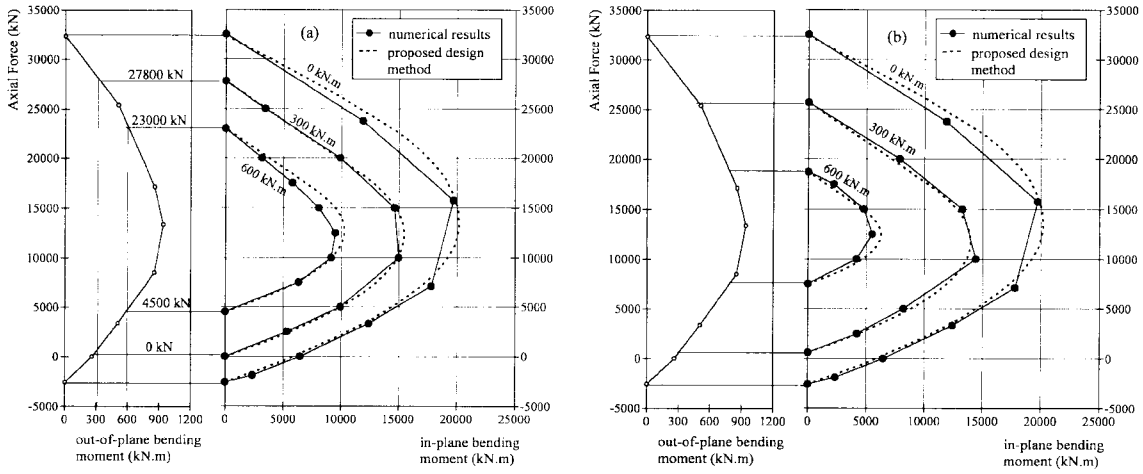

Fig. 8 Variations of intraction curve of in-plane bending moment and axial force with out-of-plane bending moments: (a) in cases when the slenderness effect is not included; (b) in cases when the slenderness effect is included

interaction curve of in-plane bending moment and axial force, with the given out-of-plane bending moments. The shape of the interaction curves is similar to that for a curve not affected by the out-of-plane bending moment. The interaction curve shrinks as the out-of-plane bending moment increases. In cases when the slenderness effect is included, the range of the permissible axial force diminishes due to the magnified out-of-plane bending moment. Accordingly, the interaction curve shrinks further. In Fig. 9, this can be observed also for a 10 meter long wall with the same properties as the 5 meter long wall.

Fig. 10 shows the profile of the internal axial force with the numerical results shown in Fig. 8(a) in the cases when the slenderness effect is not included. The internal axial forces are measured at the Gaussian points along the length at mid-height (see A-A section in Fig. 4). As noted above, the maximum and the minimum internal axial forces are determined by the magnitude of the out-of-plane bending moment. As shown in the interaction curve of the out-of-plane bending moment in Fig. 8(a), for 300 kN·m (60 kN·m/m) of the out-of-plane bending moment, the potential maximum and minimum axial forces are 27800 kN and 0 kN, respectively. The potential maximum force per unit length is 55.6 kN/cm (the maximum axial force=27800 kN; the maximum axial force per unit length=27800 kN/500 cm=55.6 kN/cm). The potential minimum force per unit length is 0 kN/cm (the minimum axial force=0 kN). As shown in Fig. 10(a), regardless of the magnitudes of the external axial force and the corresponding in-plane bending moment, the internal axial forces do not exceed both the maximum and the minimum that are defined in the interaction curve of out-of-plane bending moment and axial force. As shown in the interaction curve of the out-of-plane bending moment in Fig. 8(a), for 600 kN·m (120 kN·m/m) of the out-of-plane bending moment, the potential maximum and minimum axial forces are 23000 kN and 4500 kN, respectively. The maximum per unit length is 46 kN/cm (=23000 kN/500 cm), and the minimum per unit length is 9 kN/cm (=4500 kN/500 cm). As shown in Fig. 10(b), the internal axial forces do not exceed the maximum and the minimum, either. The figures verify that the internal axial force per unit length does not exceed the range defined in the interaction curve of the out-of-plane bending moment.

As shown in the figures, the distribution curve in the compression zone is approximately

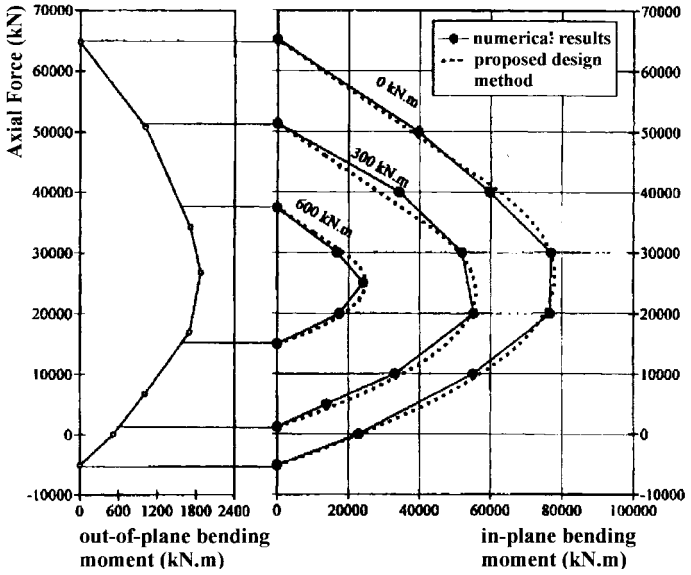

Fig. 9 Variations of interaction curve of in-plane bending moment and axial force with out-of-plane bending moments for 10 meter long wall in cases when the slenderness effect is included

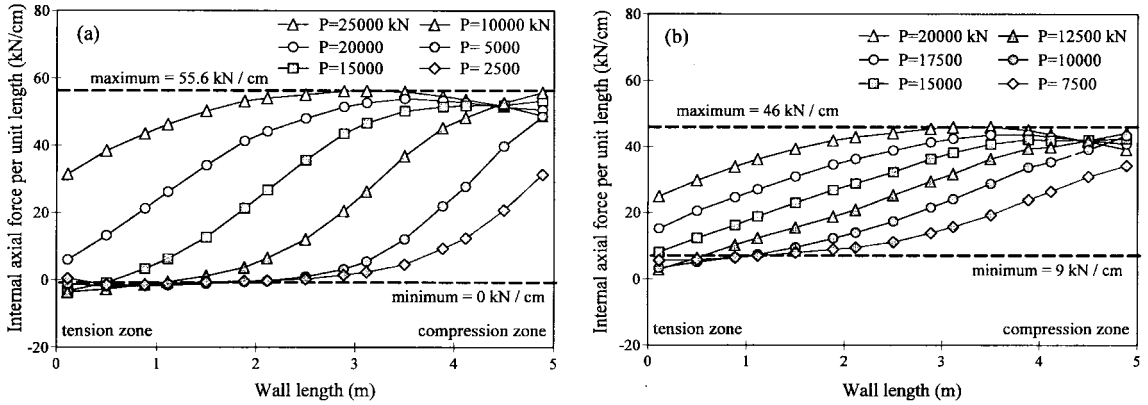

Fig. 10 Profile of distributed internal axial force; (a) Out-of-plane bending moment=300 kN·m (60 kN·m/m); (b) Out-of-plane bending moment=600 kN·m (120 kN·m/m)

parabolic. The ultimate internal force at the end in the compression zone is the maximum. The internal compressive force gradually decreases along the length toward the tension zone. Once approaching the minimum at a location, the internal axial force then becomes uniform with the minimum in the tension zone and the compression zone beyond the location. This indicates that regardless of the increase in the tensile strain beyond the location, the load capacities of the wall segments become uniform with the minimum. The minimum belongs in the range of tension control in the interaction curve. In the range of the tension control, since the yielding of reinforcing steel occurs before the compressive crushing of concrete, the behavior shows a relatively large ductility, and the ultimate strength is almost equal to the yield strength. The minimum is not necessarily a tensile force and could be a compressive force. As shown in Figs. 8(a) and 10(b), for 600 kNm

(120 kN·m/m) of the out-of-plane bending moment, the minimum is a compressive force that is 9 kN/cm.

4. Proposed method for estimating ultimate strength

The distributed internal forces should coincide with the corresponding strains. However, to estimate the distributed internal forces and the corresponding strains requires complex numerical calculations. Therefore, simple methods are required in practice for member design. In Fig. 10, the numerical results show the profile of the distributed internal force. Based on the numerical results, the distribution of the internal force can be idealized, as shown in Fig. 11. The distribution curve in the compression zone is parabolic. The ultimate force of the curve is defined by the maximum, $\overline{P}_{max}$, given in the interaction curve of out-of-plane bending moment and axial force. The internal compressive force, $\overline{P}(x)$, gradually decreases along the length toward the neutral axis. The internal axial force in the tension zone is uniform with the minimum, $\overline{P}_{min}$. If the minimum is a compressive force, the internal force then approaches the minimum in the compression zone. In the tension zone and the compression zone beyond the location, the internal force becomes uniform with the minimum.

The proposed method for estimating the ultimate strength of the wall uses the idealized distribution of the internal axial force. The procedures for the proposed method are summarized by the following steps:

1) Plot the interaction curve of out-of-plane bending moment and axial force for a wall segment with unit length.
2) In the interaction curve, determine the potential maximum and minimum of the internal axial forces corresponding to the given amount of the out-of-plane bending moment (see Fig. 12a). The maximum belongs to the range of compression control. The minimum belongs to the range of tension control.
3) In cases when the slenderness effect is included, the maximum and the minimum should correspond to the out-of-plane bending moments that are magnified by themselves. Thus, use the iterative method to determine the maximum and the minimum forces corresponding to the

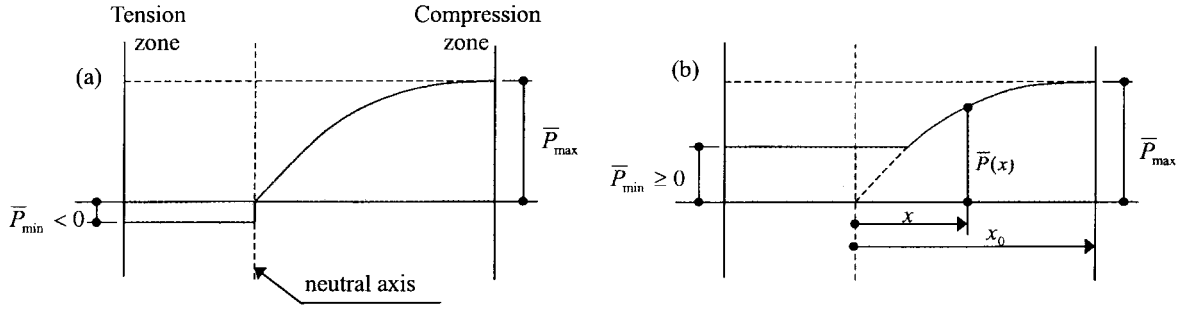

$$\overline{P}(x) = \overline{P}_{max}\left[2\left(\frac{x}{x_0}\right) - \left(\frac{x}{x_0}\right)^2\right] \geq \overline{P}_{min}$$

Fig. 11 Profile of idealized internal force: (a) $\overline{P}_{min}<0$; (b) $\overline{P}_{min} \geq 0$

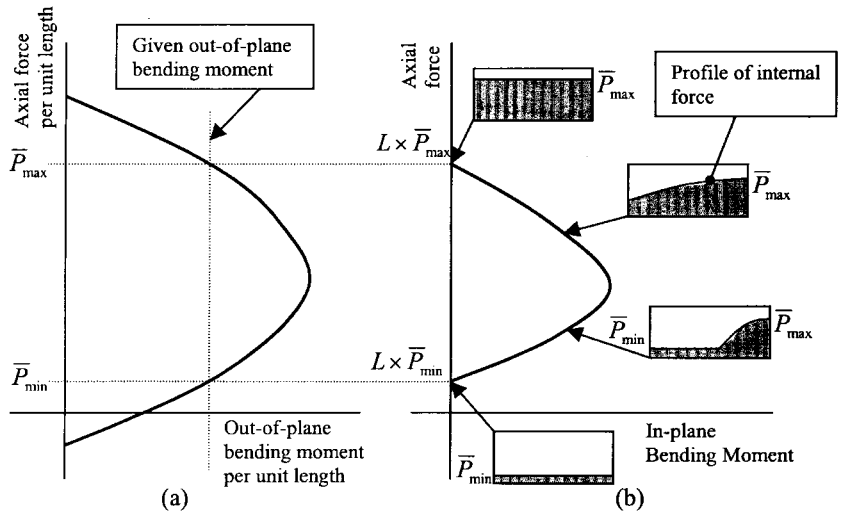

Fig. 12 Proposed method for estimating the ultimate strength of wall: (a) Potential maximum and minimum axial forces defined in the interaction curve of out-of-plane bending moment and axial force; (b) Interaction curve of in-plane bending moment and axial force

magnified out-of-plane bending moment.

4) For a given location of the neutral axis, plot the profile of the internal force as shown in Fig. 11. Then, calculate the axial force and the in-plane bending moment with respect to the centroid of the cross-section.
5) Repeat step 4) for different locations of the neutral axis. Then, plot the interaction curve of in-plane bending moment and axial force, as shown in Fig. 12(b).

5. Comparison with numerical results

Figs. 8 and 9 show the comparison of the numerical results and the interaction curves produced by the proposed method. The maximum and the minimum internal forces used in the proposed design method are obtained by the finite element analyses. As shown in Fig. 7(b), they can be obtained by either increasing or decreasing the axial force up to the ultimate strength with the uniform out-of-plane bending moment. As shown in Figs. 8 and 9, the interaction curves by the proposed method agree well with the numerical results, whether the slenderness effect is included or not.

6. Comparison with existing method

In Figs. 13 and 14, the interaction curves from the proposed method and PCACOL(Portland Cement Association 1992) are compared. PCACOL uses the general assumption that strains in the cross section shall be directly proportional to the distance from the neutral axis. The interaction curve of out-of-plane bending moment and axial force used in the proposed method is given by PCACOL. Figs. 13 and 14 show the interaction curves without and with slenderness effect,

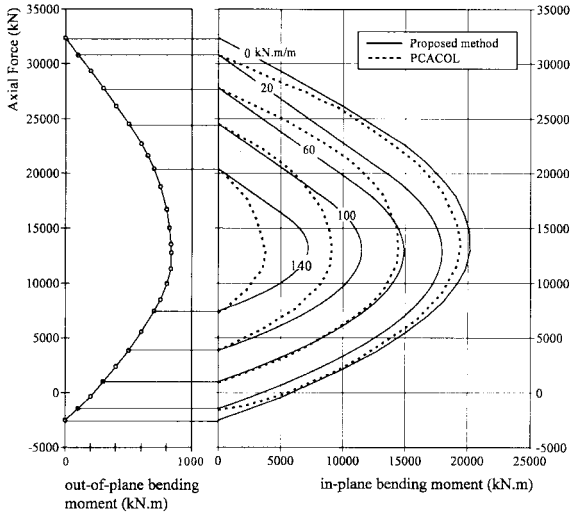

Fig. 13 Comparison of interaction curves by proposed method and by PCACOL in cases when the slenderness effect is not included

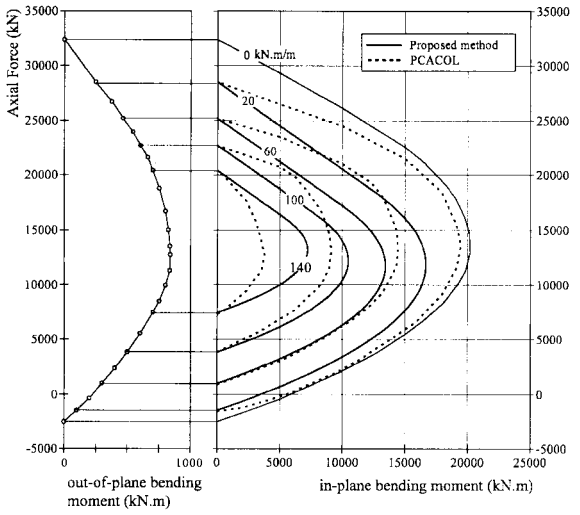

Fig. 14 Comparison of interaction cueves by proposed method and by PCACOL in cases when the slenderness effect is included

respectively. In cases when the slenderness effect with respect to the out-of-plane bending is included, the moment magnification factor in ACI 318-95 is used.

$$\delta=\frac{C_m}{1-\frac{P_u}{P_c}} \geq 1.0, \text{ where } P_c=\frac{\pi^2 EI}{(kl_u)^2} \tag{4}$$

It is assumed that C_m=0.4, k=0.8, l_u=4.0m, EI=0.4E_cI_g, and E_c=4700$\sqrt{f_c'}$. With the constants, P_c is approximately equivalent to 34000 kN (68 kN/cm). In PCACOL, the moment magnification factor is calculated with P_u which is the external axial force. In the proposed method, on the other hand, the moment magnification factor is calculated at the wall segment at the compression end.P_u is the maximum internal force corresponding to the given out-of-plane bending moment.

As shown in Fig. 13, compared with the proposed method, PCACOL overestimates the ultimate strength for low out-of-plane bending moments, while it underestimates the ultimate strength for high out-of-plane bending moments. As shown in Fig. 14, in cases when the slenderness effect is included, there is a wide difference between the ultimate strengths given by the proposed method and by PCACOL. In PCACOL, under 20000 kN of the external axial force, the moment magnification factor is 1.0 so the slenderness effect is not included. In the proposed method, the out-of-plane moment in the compression zone is magnified by the internal axial force that is larger than the external axial. Therefore, the slenderness effect appears even under 20000 kN of the external axial force.

This example does not indicate that the moment magnification factor in Eq. (4) is applicable to the actual local buckling that is a complex mechanism. However, if the local buckling strength at the maximum internal force of the wall segments can be defined precisely, then the strength of the slender wall under combined axial force and biaxial bending moments can be determined by the proposed design method.

7. Conclusions

Numerical studies using nonlinear finite element analysis were done for investigating the behavior of isolated reinforced concrete walls subjected to combined axial force and in-plane and out-of-plane bending moments. For nonlinear finite element analyses, a computer program addressing material and geometric nonlinearities was developed.

Through numerical studies, the distribution of the internal force over the cross-sections of walls was investigated. The numerical results reveal that: (1) the range of the internal axial force per unit length depends on the given amount of the out-of-plane bending moment; (2) the potential maximum and minimum of the internal axial force per unit length can be determined in the interaction curve of out-of-plane bending moment and axial force; and (3) the maximum belongs to the range of compression control, whereas the minimum belongs to the range of tension control.

Based on the numerical results, the distribution of the internal force was idealized. Then, a new method for estimating the ultimate strength of the wall was developed. According to the proposed method, variations in the interaction curve of in-plane bending moment and axial force depends on the range of the permissible axial force per unit length that is determined by the given amount of the out-of-plane bending moment. As the out-of-plane bending moment increases, the interaction curve shrinks, which indicates a decrease in the ultimate strength.

The proposed method is not based on the plane section hypothesis, so it was compared with an existing method based on the plane section hypothesis. The comparison has shown that the plane section hypothesis can lead to an inaccurate estimation of the ultimate strength of the wall. Compared with the proposed method, the existing method overestimates the ultimate strength for low out-of-plane bending moments, but it also underestimates the ultimate strength for high out-of-plane bending moments. For slender walls, there is a wide difference between the ultimate strengths given by the proposed method and that by the existing method.

Obviously, current design methods based on the plane section hypothesis can not address the out-of-plane local behavior of an individual wall segment, including local buckling that may govern the ultimate strength of the entire wall. On the other hand, the proposed method provides a reasonable approach that can address the out-of-plane local behavior of the wall segments.

The proposed method can be used only for isolated walls with uniformly distributed reinforcements. Further studies are required for walls with different conditions.

References

American Concrete Institute (1995), "Building code requirements for structural concrete", *ACI 318-95*, Detroit, 118-121, 227-230.

Aoyama, H. and Yoshimura, M. (1980), "Tests of RC shear walls subjected to biaxial loading", *Proc., 7th World Conf. on Earthquake Engrg.*, Turkish National Committee on Earthquake Engineering, Istanbul, Turkey, 511-518.

Bathe, K. (1982), *Finite Element Procedures in Engineering Analysis*, Prentice-Hall, Inc, 301-406.

Huria, V., Raghavendrachar, M. and Aktan, A.E. (1991), "3-D characteristics of RC wall response", *J. Struct. Engrg., ASCE*, **117**(10), 3149-3167.

Park, H. and Klingner, R.E. (1997), "Nonlinear analysis of RC members using plasticity with multiple failure criteria", *J. Struct. Engrg., ASCE*, **123**(5), 643-651.

Park, H. (1999), "Numerical study on RC flat plates subjected to combined axial and transverse load", *Structural*

Engineering and Mechanics, An Int. J. **8**(2), 137-150.
Portland Cement Association (1992), PCACOL, *Strength Design of Reinforced Concrete Column Sections*.
Weaver, Jr., W. and Johnston, P.R. (1984), *Finite Elements for Structural Analysis*, Prentice-Hall Inc, 236-254.

Notation

The following symbols are used in this paper:

A_s = area of reinforcing steel bar;
e_1 = eccentricity with respect to in-plane bending;
e_2 = eccentricity with respect to out-of-plane bending;
E_c = the modulus of elasticity of concrete, MPa;
f_i = failure criterion;
f_c' = concrete cylinder strength;
g_i = effective stress;
I_g = moment inertia of gross concrete section about centroidal axis;
J_2 = second deviatoric stress invariants;
k = effective length factor for compression members;
l_u = unsupported length of compression member;
L = length of wall;
P_u = external axial force;
P_c = critical force;
$\bar{P}(x)$ = internal axial force per unit length at x along the length of wall;
$\bar{P}_{\max}$ = potential maximum axial force per unit length;
$\bar{P}_{\min}$ = potential minimum axial force per unit length;
x = distance from neutral axis;
x_0 = distance from compression end to neutral axis;
$\Delta\underline{\varepsilon}_p$ = total incremental plastic strain vector;
$\Delta\underline{\varepsilon}_{pi}$ = incremental plastic strain vector of compressive crushing or tensile cracking;
δ = moment magnification factor;
σ = hydrostatic pressure; and
$\bar{\sigma}_i$ = function of the failure surface.